J. C. Newman, K. N. Shivakumar†, and D. E. McCabe‡*

Finite Element Fracture Simulation of A533B Steel Sheet Specimens

REFERENCE Newman, J. C., Shivakumar, K. N., and McCabe, D. E., **Finite element fracture simulation of A533B steel sheet specimens**, *Defect Assessment in Components – Fundamentals and Applications*, ESIS/EGF9 (Edited by J. G. Blauel and K.-H. Schwalbe) 1991, Mechanical Engineering Publications, London, pp. 117–126.

ABSTRACT An elastic–plastic finite-element analysis was used to model stable crack growth behaviour in compact C(T) specimens and to predict fracture behaviour in middle-crack tension M(T) specimens made of A533B steel sheet. The crack-growth criteria studied were the critical crack-tip opening displacement (CTOD) or angle (CTOA) criterion, the J–R resistance curve, and a CTOD resistance curve. The crack-mouth-opening displacement against crack extension (COD-Δa) test results were also used as input to the finite element analysis, in a so-called generation mode, to study the CTOD variations during crack extension.

Calculated results using the critical CTOD (or CTOA) criterion on compact specimens agreed well with test data up to maximum load, but tended to predict slightly larger crack extensions and predict larger load-line displacements than test results beyond maximum load. Analyses using the critical CTOD criterion predicted maximum loads on various M(T) specimens 4–7 percent lower than tests. Using J or CTOD resistance curves, the analyses also predicted lower maximum loads on the M(T) specimens (3–5 percent). The generation-mode analyses indicated that CTOD on both specimens types varied with crack extension but was nearly constant after about 5 mm of crack extension. Under the generation mode, comparisons made between contour and deformation J values from tests and analyses agreed well. Similarly, a comparison between δ_5 (CTOD at the initial fatigue crack-tip location) from test and analysis also agreed well. A normalized J parameter (linearly proportional to load) plotted against crack extension gave nearly the same resistance curve for both C(T) and M(T) specimens.

Introduction

The phenomenon of stable crack growth has been studied extensively using elastic–plastic finite element methods **(1)–(10)**. These studies were first conducted to develop efficient techniques to simulate crack extension and to later examine various local and global fracture criteria. Some of these criteria were crack-tip stress or strain, crack-tip-opening displacement or angle, crack-tip force, energy release rates, J integral **(11)(12)**, and tearing modulus **(13)**. Consistent among many of these investigations is that CTOA (or CTOD at a specified distance from the crack tip) was most suited for modeling stable crack growth and instability during the fracture process. CTOA (or CTOD) approached nearly a constant value after some amount of crack extension. However, during the phase between initiation and the attainment of maximum load, CTOA (or CTOD) did not appear to be constant for some materials **(7)(8)**.

* Materials Division, NASA Langley Research Center, Mailstop 188E, Hampton, Virginia, 23665, USA.
† Analytical Services and Materials, Inc., Hampton, Virginia, 23666, USA.
‡ Materials Engineering Associates, Inc., Lanham, Maryland, 20706, USA.

Experimentally, Luxmoore *et al.* **(14)** have shown that CTOA (or CTOD) was nearly constant from the onset of stable crack growth in two aluminum alloys, but was dependent upon crack configuration. Paleebut **(15)**, using a laser-interferometric displacement gauge on compact specimens, measured CTOD at initiation of stable crack growth on two aluminum alloys. The measured CTOD values agreed well with the critical CTOD values used by Newman **(10)** to fit initiation and stable crack growth behavior up to maximum load on the same materials.

The purpose of this paper is to further evaluate CTOD and J resistance curve criteria for modeling stable crack growth in thin-sheet material using an elastic–plastic finite element analysis. A two-dimensional plane-stress analysis was used to model stable crack growth in compact C(T) and in middle-crack tension M(T) specimens made of A533B steel sheet material. First, a critical crack-tip opening displacement (CTOD) at a specified distance (d) from the crack tip, or equivalently, a critical crack-tip opening angle (CTOA) was found that would accurately model stable crack growth in a C(T) specimen. The same critical CTOD value was then used to predict crack extension, load–line displacements, and maximum load on various size M(T) specimens. A J–R resistance curve and a CTOD resistance curve, determined from the C(T) specimen, was also used to predict the fracture behaviour of the M(T) specimens. In addition, the remote crack-mouth-opening displacement against crack extension (COD-Δa) test results were used as input in the finite-element analysis to study CTOD variations during crack extension. This latter approach is often referred to as a generation-mode analysis. Some comparisons are made between δ_5 (CTOD at the initial fatigue crack-tip location **(16)**) and J from tests and from generation-mode analyses. The sensitivity of J and CTOD to load for the A533B sheet material is discussed.

Finite element analyses

The elastic–plastic analysis of the two specimen types employed the finite element method and the initial stress concept to implement the elastic–plastic analysis **(10)(17)**. The analysis was based on incremental flow theory with a small strain assumption. A multi-linear representation of the uniaxial stress–strain curve was used in the analysis with the von Mises yield criterion. The finite element models for these specimens were composed of two-dimensional, constant strain, triangular elements under plane-stress conditions. Mesh patterns were selected so that the minimum element size along the line of crack extension would be the same in all specimens. From previous studies **(10)**, a mesh size (d) of 0.8 mm, in the crack-tip region, was selected. CTOD was measured at the first node along the crack surface from the crack tip ($d = 0.8$ mm). The particular meshes used for the C(T) and M(T) specimens are shown in reference **(10)**. The C(T) specimen had 2091 nodes and 3848 elements; whereas, the M(T) specimen had 949 nodes and 1739 elements. (The elastic compliance of the models, C(T) and M(T), were about 2 percent lower than accepted solutions from the literature.) Fictitious springs were used to change boundary conditions associated with crack extension. For free nodes along the crack line, the spring stiffnesses were set equal to zero; and for fixed nodes, the stiffnesses were assigned extremely large values. (See reference **(10)** for details on the finite element analysis with crack extension.)

During incremental analyses under displacement control, the stiffness of the crack-tip spring was set equal to zero if the specified crack-extension criterion was satisfied and the crack advanced to the next fixed node. This process was repeated until the desired crack length was reached.

Experiments

The experiments were conducted at the Westinghouse Research and Development Laboratory by D. E. McCabe. The material was A533B steel sheet ($B = 2.5$ mm thick) with a yield stress (σ_{ys}) and ultimate tensile strength (σ_u) of 470 and 620 MPa, respectively. The strain hardening coefficient, n, was about 10. Tests were conducted on compact specimens ($w = 203$ mm) with an initial crack-length-to-width ratio, a_i/w, of 0.5 and on middle-crack tension specimens (half-width, w, of 102 and 203 mm) with a_i/w values of 0.5–0.6. Both specimens were restrained from buckling by guide plates. Crack extension was measured by both the compliance and visual methods on the C(T) specimens but only the visual method was used for the M(T) specimens. The δ_5 (CTOD at the initial fatigue crack-tip location) was measured only on the M(T) specimens. Crack-mouth-opening (load–line) displacements (COD) were measured on all specimens. For the C(T) specimen, COD was measured on the crack line directly under the load line. On the M(T) specimen, COD was measured along the load centreline with a total gauge length of $1.25w$. J-integrals were calculated from deformation theory using load–line displacement records for both specimen types **(18)**.

Results and discussion

A compact specimen was initially analyzed under plane-stress conditions to determine the critical CTOD value ($\delta_c = 0.19$ mm) that would cause the analysis to match the experimental maximum load carried by the specimen. The experimental and calculated load-against-crack-extension (P-Δa) results are shown in Fig. 1. Experimental crack extension values, measured by unloading compliance or visual methods, are shown as symbols. Beyond maximum load, the CTOD criterion (solid curve) tended to predict slightly larger crack-extension values for a given load. The dashed–dot curve shows the P-Δa calculations from the COD-Δa generation-mode (GM) analysis. (The COD-Δa input data was obtained from the compact specimen by averaging the crack extensions from compliance and visual observations.) The analysis using the COD-Δa mode tended to predict higher loads for a given amount of

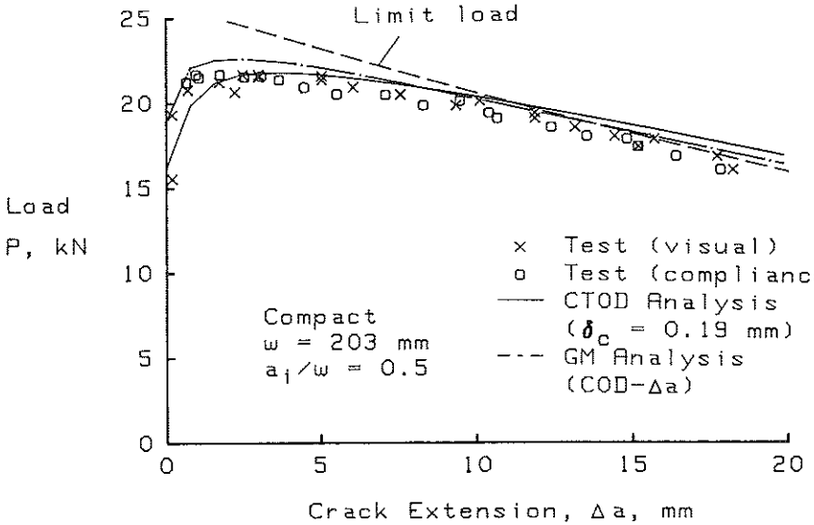

Fig 1 Comparison of load against crack extension from test and analysis for compact specimen

crack extension probably because the model is slightly stiffer than the actual specimen. The dashed curve shows the limit-load condition for comparison. The limit load was calculated from a plastic-hinge analysis by Newman **(19)** assuming no crack-tip constraint and using the ultimate tensile strength. The limit load (P_L) was given by

$$P_L = \sigma_u Bw(1-\lambda)\{[1+(1+\lambda)^2/(1-\lambda)^2]^{1/2} - (1+\lambda)/(1-\lambda)\} \quad (1)$$

where $\lambda = a/w$. Equation (1) is identical to that independently developed by Merkle and Corten **(20)**, except that the ultimate tensile strength is used instead of the yield stress. Figure 2 shows comparisons among the experimental and numerical load against load–line displacements for the compact specimen. The results from the CTOD criterion agreed well with the test results except beyond maximum load (COD > 8 mm). The COD-Δa generation mode results (P-Δa and P-COD) agreed reasonably well with test data, but the predicted maximum load was 4 percent too high. The CTOD variation with crack extension from the generation mode analyses will be discussed later.

To test the CTOD criterion, the fracture behaviour of the M(T) specimens was predicted from the analysis using a critical CTOD value of 0.19 mm, as determined from the C(T) specimen. Typical comparisons between the CTOD analysis (solid curve) and test data (symbols) are shown in Figs 3 and 4 for P-Δa and P-COD results, respectively. The CTOD analysis predicted the same trend as the test data but the predicted load for a given amount of crack extension or displacement was as much as 6 percent lower. The dashed curve in Fig. 3 is the limit load calculated by $P_L = \sigma_u Bw(1 - a/w)$. The dash–dot

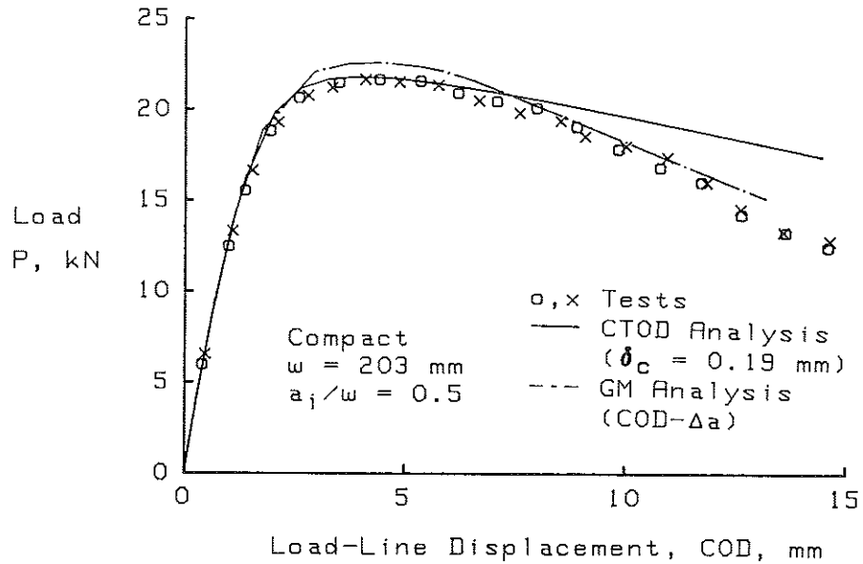

Fig 2 Comparison of load against load–line displacement from test and analysis for compact specimen

curves in Figs 3 and 4 show predictions from a J–R curve analysis using a J–R curve that was determined from the compact specimen. Results from the J–R curve analyses were quite similar to those from the CTOD criterion. However, the J–R curve analysis predicted slightly higher maximum loads than the

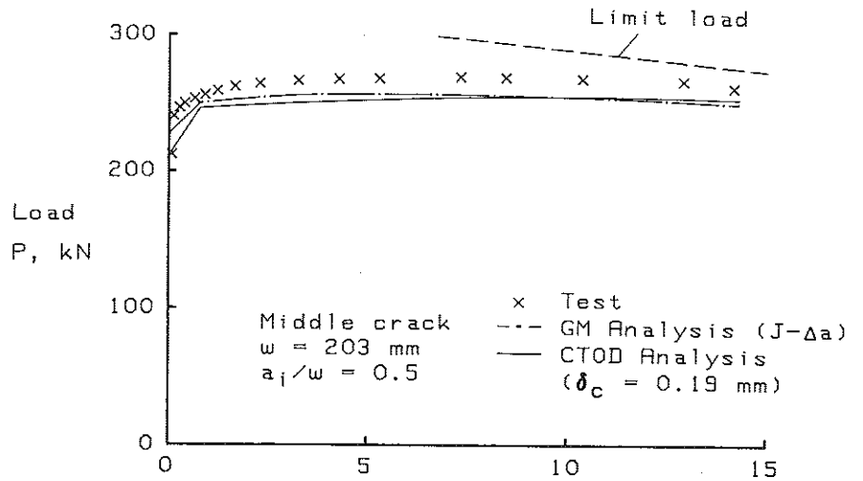

Fig 3 Comparison of load against crack extension from test and analyses for middle-crack tension specimen

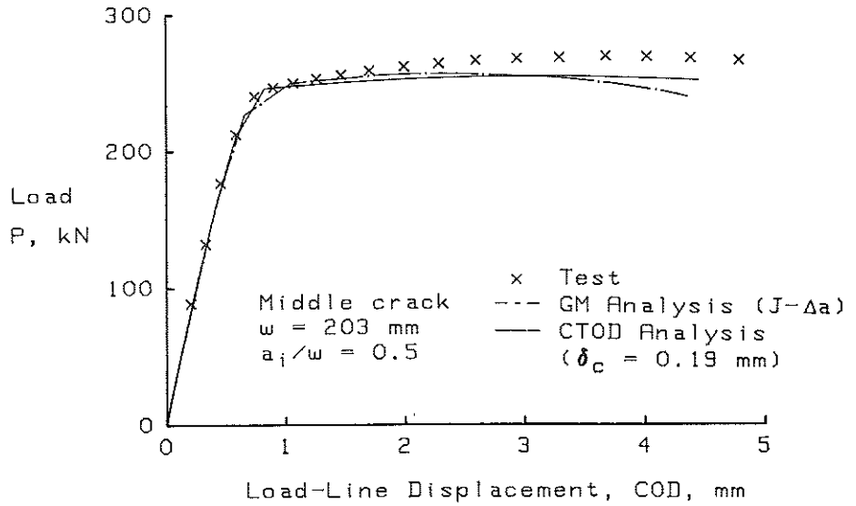

Fig 4 Comparison of load against load–line displacement from test and analyses for middle-crack tension specimen

CTOD criterion (about 5 percent lower than tests) but tended to underestimate loads for large amounts of load–line displacement (COD > 3 mm). (Results from a CTOD resistance curve, not shown, gave similar results as the *J–R* curve analysis but did not show the same drop in load for large amounts of displacement.)

The COD-Δ*a* generation mode analysis of the M(T) specimen gave a reasonably good fit to the *P*-Δ*a* and *P*-COD test data (not shown). However, the CTOD variation with crack extension from this analysis is shown in Fig. 5 for the M(T) specimen (dash–dot curve). For comparison, the results from the generation-mode analysis of the C(T) specimen is shown by the solid curve. The initiation CTOD values were quite close for both specimen types, but large variations in CTOD with crack extension were observed for both specimen types. However, the CTOD values tend to level off after about 5 mm of crack extension (about twice the specimen thickness). The CTOD values for the M(T) specimen were generally higher than those from the C(T) specimen. For the A533B material, CTOD is very sensitive to load because the strain-hardening coefficient, *n*, is about 10. The large variations (factor of 3 on each specimen) shown in Fig. 5 result from small changes in load. Recall that the constant CTOD analysis predicted maximum loads on M(T) specimens within 4 to 7 percent. The dashed line shows the constant CTOD value (0.19 mm) that was used in the constant CTOD simulation.

It is interesting to note that for both the C(T) and M(T) specimens, the COD-Δ*a* simulation gives nearly constant CTOD values after crack extensions of about twice the thickness. A possible reason for the large variation in

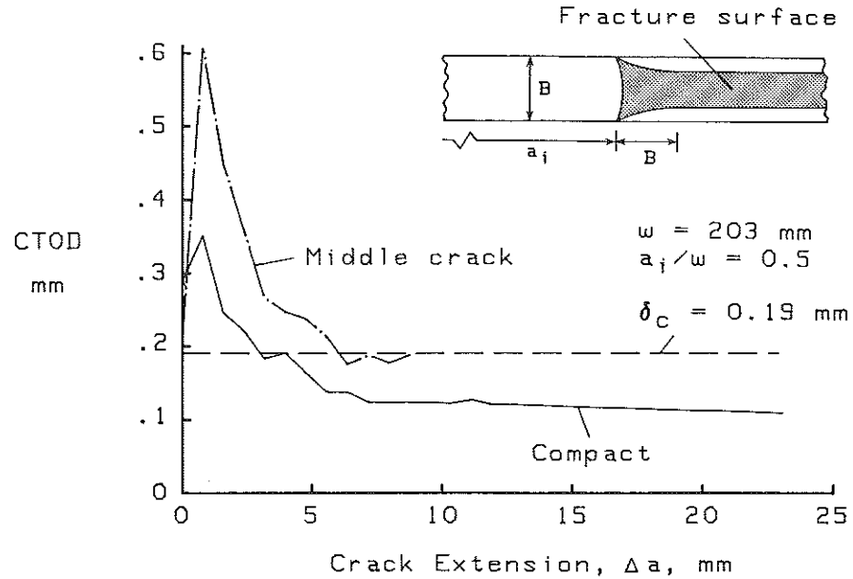

Fig 5 Numerical CTODs for compact and middle-crack tension specimens from COD-Δ*a* generation-mode analyses

CTOD for Δ*a* < 5 mm may be due to the changes in triaxial constraint as a virgin crack grows into a highly deformed region. As the crack grows, the material ahead of the crack front undergoes a large reduction in thickness while the material behind the crack front is nearly unaffected by the intense deformation (see insert in Fig. 5). This change in the deformed shape should induce a triaxial constraint that is not captured by the two-dimensional analysis. A large deformation, three-dimensional analysis would be required to capture the influence of this intense deformation on crack-tip behaviour.

Figures 6 and 7 show comparisons of test measurements (symbols) and numerical calculations of δ_5 and *J* under the COD-Δ*a* generation-mode analyses, respectively. The δ_5 measurements and calculations (Fig. 6) were obtained for a total gauge length of 5 mm at the initial crack-tip location. The calculations agreed well with test data. The measured and calculated *J–R* curves (Fig. 7) were found to be dependent upon specimen type. The M(T) specimens gave higher *J–R* curves than the C(T) specimens. This large difference between specimen types, however, will be shown later to be due to a small change in applied load. These comparisons between test and analyses do show that the two-dimensional analyses (with the 0.8 mm size elements) are able to accurately model the in-plane deformations for the A533B sheet material.

The large variation in *J–R* curves, shown in Fig. 7, is similar to the CTOD variations shown in Fig. 5. The *J*-integral, like CTOD, is also quite sensitive to

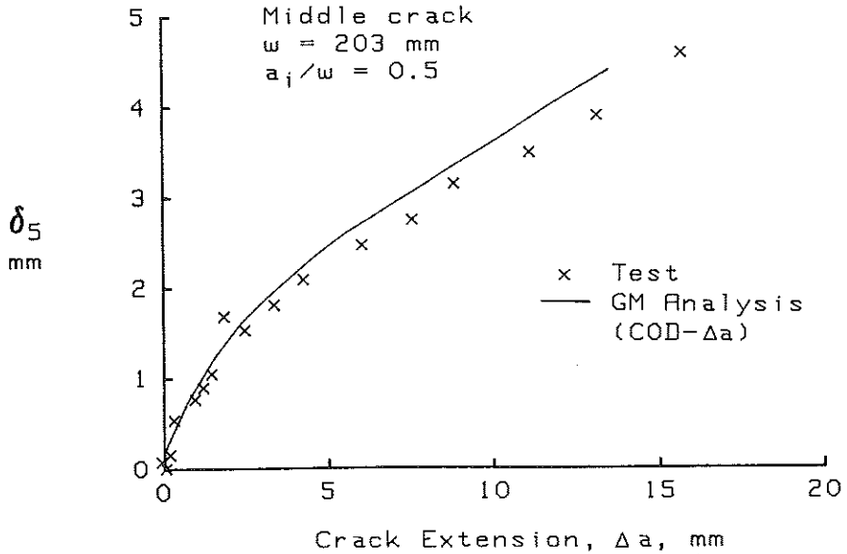

Fig 6 Comparison of initial fatigue crack-tip CTOD, δ_5, from test and analysis for middle-crack tension specimen

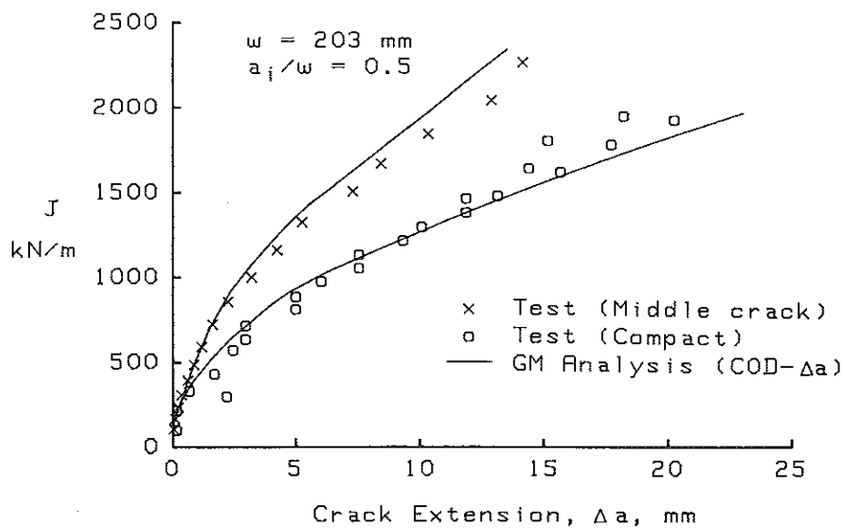

Fig 7 Comparison of deformation J (test) and contour J (analysis) from COD-Δa generation-mode analyses

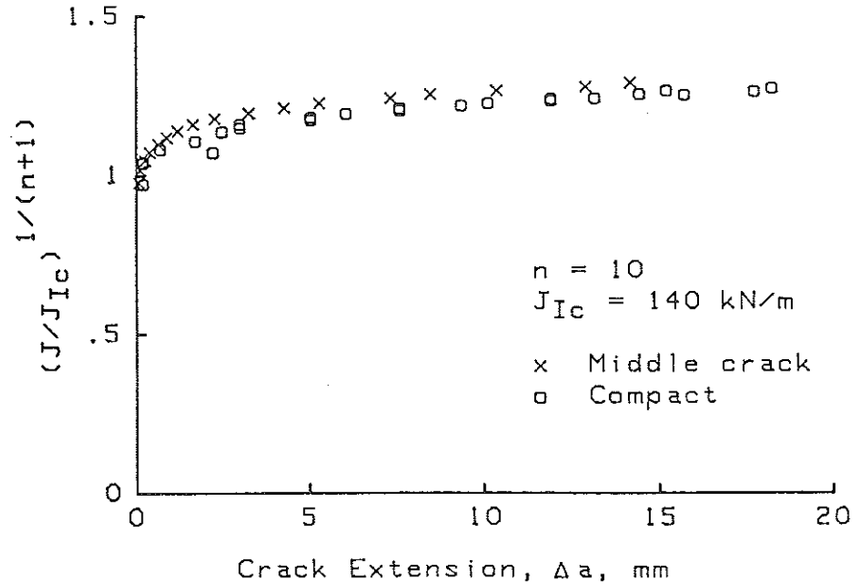

Fig 8 Comparison of normalized J parameter (linearly proportional to load) from tests of compact and middle-crack tension specimens

load. For power-law hardening materials, Hutchinson **(21)** has shown that the crack-tip stress field is proportional to $J^{1/(n+1)}$, where n is the power-law hardening coefficient. Therefore, if the local stress field controls the fracture process in the C(T) and M(T) specimens, then the parameter $J^{1/(n+1)}$ may be the same for a given amount of crack extension. This parameter is also linearly proportional to load **(22)**. Figure 8 shows a comparison of normalized J raised to the $1/(n+1)$ power plotted against crack extension for the C(T) and M(T) specimens. The two data sets collapse together quite well (within about 4 percent). This indicates that large differences in J and CTOD may be caused by only small changes in load. From a structural design viewpoint, the correlation in Fig. 8 is quite satisfactory. In fact, this form shows that A533B sheet material has very little load carrying capacity beyond J_{Ic}. Also, the initiation toughness, J_{Ic}, can be more readily identified in Fig. 8 than in Fig. 7.

Conclusions

Two-dimensional plane-stress fracture simulations on A533B steel sheet compact and middle-crack tension specimens support the following conclusions.

(1) After maximum load, the critical CTOD (or CTOA) criterion tended to predict larger crack extensions and load–line displacements in compact specimens.

(2) Analyses using a critical CTOD (or CTOA) value determined from a compact specimen predicted maximum loads on middle-crack tension specimens within 4 to 7 percent.
(3) Analyses using COD-Δa test results as input indicated that CTOD on compact and middle-crack tension specimens varied with crack extension but CTOD was nearly constant after about 5 mm of crack extension on each specimen.
(4) Analyses using J and CTOD resistance curves determined from a compact specimen predicted maximum loads on middle-crack tension specimens within 3 to 6 percent.
(5) The parameter, $J^{1/(n+1)}$, correlated crack-extension data on compact and middle-crack tension specimens within about 4 percent.
(6) All of the fracture criteria (CTOD, J, and CTOD resistance curves) that were used with two-dimensional elastic–plastic finite-element analyses accurately predicted the fracture behaviour of tension loaded specimens.

References

(1) KOBAYASHI, A. S., CHIU, S. T., and BEEUWKES, R. (1973) *Engineering Fracture Mechanics*, **5**, No. 2, 293–305.
(2) ANDERSON, H. (1973) *J. Mech. Phys. Solids*, **21**, 337–356.
(3) LIGHT, M. F., LUXMOORE, A., and EVANS, W. T. (1975) *Int. J. of Fracture*, **11**, 1045–1046.
(4) ROUSSELIER, G. (1977) *Fourth international conference on fracture*, Vol. 3, 1–6.
(5) de KONING, A. U. (1977) *Fourth international conference on fracture*, Vol. 3, 25–32.
(6) NEWMAN, J. C., Jr. (1977) *ASTM STP 637*, pp. 56–80, ASTM, Philadelphia.
(7) SHIH, C. F., de LORENZI. H. G., and ANDREWS, W. R. (1979) *ASTM STP 668*, pp. 65–120, ASTM, Philadelphia.
(8) KANNINEN, M. F., RYBICKI, E. F., STONESIFER, R. B., BROEK, D., ROSENFIELD, A. R., and HAHN, G. T. (1979) *ASTM STP 668*, pp. 121–150, ASTM, Philadelphia.
(9) SHIH, C. F. and GUDAS, J. P. (1983) *Elastic–plastic fracture ASTM STP 803*, ASTM, Philadelphia.
(10) NEWMAN, J. C., Jr. (1984) *ASTM STP 833*, pp. 93–117, ASTM, Philadelphia.
(11) RICE, J. R. (1968) *J. Appl. Mechs., Trans. ASME*, **90**, No. 2, 379–386.
(12) CHERPANOV, G. P. (1967) *USSR J. Appl. Math. and Mechs., Trans.*, **31**, 504.
(13) PARIS, P. C., TADA, H., ZAHOOR, A., and ERNST, H. (1979) *ASTM STP 668*, pp. 5–36, ASTM, Philadelphia.
(14) LUXMOORE, A., LIGHT, M. F., and EVANS, W. T. (1977) *Int. J. of Fracture*, **13**, 257–259.
(15) PALEEBUT, S. (1978) CTOD and COD measurements on compact tension specimens of different thicknesses, M.S. Thesis, Michigan State University.
(16) HELLMAN, D. and SCHWALBE, K.-H. (1984) *ASTM STP 833*, pp. 577–605, ASTM, Philadelphia.
(17) ZIENKIEWICZ, O. C., VALLIAPPAN, S., and KING, I. P. (1969) *Int. J. for Numerical Methods in Engineering*, **1**, 75–100.
(18) ERNST, H. A., PARIS, P. C., and LANDES, J. D. (1981) *ASTM STP 743*, 476–506.
(19) NEWMAN, J. C., Jr. (1974) Plane-stress fracture of compact and notch-bend specimens, NASA TMX-71926, March.
(20) MERKLE, J. G. and CORTEN, H. T. (1974) *J. Pressure Vessel Tech., Trans. ASME*, 286–292.
(21) HUTCHINSON, J. W. (1968) *J. Mechs. Phys. Solids*, **16**, 13–31.
(22) KUMAR, V., GERMAN, M. D., and SHIH, C. F. (1983) *ASTM STP 803*, I306–I353.